Title
Site-Selective Acylation of Natural Products with BINOL-Derived Phosphoric Acids

Journal
ACS Catalysis, 9(11)

ISSN
2155-5435

Authors
Li, Junqi
Grosslight, Samantha
Miller, Scott J
et al.

Publication Date
2019-11-01

DOI
10.1021/acscatal.9b03535

Peer reviewed

Published in final edited form as:

ACS Catal. 2019 November 1; 9(11): 9794–9799. doi:10.1021/acscatal.9b03535.

Site-selective acylation of natural products with BINOL-derived phosphoric acids

Junqi Li[§,†,#,⊥], **Samantha Grosslight**[§,‡], **Scott J. Miller**[*,#], **Matthew S. Sigman**[*,‡], **F. Dean Toste**[*,†]

[†]Department of Chemistry, University of California, Berkeley, California 94720, United States

[‡]Department of Chemistry, University of Utah, 315 South 1400 East, Salt Lake City, Utah 84112, United States

[#]Department of Chemistry, Yale University, New Haven, Connecticut 06520-8107, United States

Abstract

The site-selective acylation of a steroidal natural product 19-hydroxydehydroepiandrosterone catalyzed by 1,1'-Bi(2-napthol)-derived (BINOL) chiral phosphoric acids (CPA's) is described. Systematic variation and multivariate linear regression analysis reveal that the same steric parameters typically needed for high enantioselectivity with this class of CPAs are also required for site-selectivity in this case. Density functional theory calculations identify additional weak CH-π interactions as contributors to site discrimination. We further report a rare example of site-selective acylation of phenols through the evaluation of naringenin, a flavonoid natural product, using CPA catalysis. These results suggest that BINOL-derived CPA's may have broader applications in site-selective catalysis.

Graphical Abstract

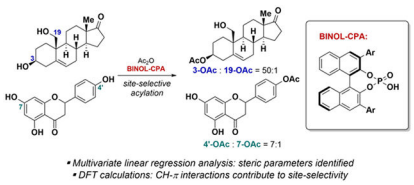

Keywords

Site-selective catalysis; acylation; chiral phosphoric acids; modeling; non-covalent interactions

[*]**Corresponding Author**: F. Dean Toste: fdtoste@berkeley.edu, Matthew S. Sigman: sigman@chem.utah.edu, Scott J. Miller: scott.miller@yale.edu.

[§]These authors contributed equally.

[⊥]Department of Chemistry, Iowa State University, Ames, Iowa 50011, United States

Supporting Information

The Supporting Information is available free of charge on the ACS Publications website.

Experimental details, procedures, compound characterization data, computational details, and copies of NMR spectra of new compounds (PDF).

X-ray crystallographic data for **6** (CIF)

The authors declare no competing financial interests.

Chiral phosphoric acids (CPAs) and phosphates based on the BINOL scaffold have been used extensively for a myriad of asymmetric transformations,[1] indicating their ability to effectively induce significant energetic differences between diastereomeric transition states across different reaction manifolds. Similarly, site-selective functionalization of natural products requires significant energetic differentiation between structurally distinct transition states, with the additional challenge of overcoming innate selectivity.[2] Despite their successful employment as asymmetric catalysts, there have been limited cases of using BINOL-derived phosphoric acids in selective natural product modifications. Notably, Nagorny and co-workers demonstrated that CPAs are capable of distinguishing between different alcohols on polyketide antibiotics for site-selective glycosylation,[3] and others have reported that CPAs can be effective for site-selective acetalizations of compounds with more than one hydroxyl group.[4] Other classes of organocatalysts have been used in both enantio- and site-selective acyl transfers, such as peptides,[5,6] borinic[7] and boronic acids,[8] covalent scaffolding catalysts,[9] and *N*-heterocyclic carbenes.[10] Chiral metal complexes have also been employed.[11] These precedents suggest that the same catalyst features enabling asymmetric induction may be translated to site-recognition in complex molecule settings. Furthermore, site-selective functionalization with CPAs may be achievable through strategic manipulation of the noncovalent substrate-catalyst interactions known to be crucial for asymmetric induction with CPAs.[12] Herein, we report the site-selective acylation of two natural products using BINOL-derived CPAs as catalysts and demonstrate that the same catalyst features characteristically required for high enantioselectivity also enable high site-selectivity.

We first examined the site-selective acylation of 19-hydroxy-(**1**, 19-OH-DHEA), a steroidal natural product with a hydrocarbon backbone. Evaluation of the acylation of **1** under common acylating conditions revealed that the secondary and primary alcohols in the neopentyl framework have comparable innate reactivity (Table 1, Entries 1-2). Inspired by Takasu's report on the kinetic resolution of alcohols catalyzed by BINOL-derived phosphoric acids,[13,14] we subjected **1** to acidic acylating conditions under the influence of catalyst **5a** (Ar = 2,4,6-tricyclohexylphenyl, TCYP), which led to an increase in selectivity, from 1.2:1 to 8.5:1 in favor of acylation of the secondary alcohol.[15] In this case, the chirality of the catalyst influences reactivity and selectivity – both the (*S*)-enantiomer of the catalyst **5b** and an achiral counterpart, **5c** gave lower selectivity (Table 1, Entries 3-5). Notably, **5b** is also a less active catalyst, giving a lower yield of the acylated products compared to 73% yield with the "matched" catalyst **5a**. Further optimization of the reaction conditions resulted in a 15:1 selectivity when catalyst **5a** (Table 1, entry 6).

Since site-selectivity is determined by the relative energy barriers of the two competing acylation pathways originating from the two alcohols,[16] we reasoned that multivariate linear regression (MLR) analysis previously adopted for studying BINOL-derived phosphoric acid-catalyzed enantioselective reactions[12d, 17] could be applied here to identify catalyst features contributing to site-selectivity. Thus, we evaluated the acylation reaction with a panel of catalysts containing different substitution patterns at the R^1-R^3 positions from which we identified catalysts giving site-selectivities of up to 50:1 (Figure 1A).

To define the catalyst parameters important for selectivity, density functional theory (DFT) optimizations were performed for the catalyst panel at the M06-2X/def2-TZVP level of theory.[12d, 17] From these optimized geometries, we collected steric and electonic parameters including Sterimol values, natural bond orbital (NBO) charges and infrared (IR) vibrations (see Supporting Information for all parameters collected).[18, 19] Comparing the collected parameters to the measured site selectivity using a step-wise linear regression algorithm revealed a statistical correlation (R^2= 0.92, intercept = 0.07) with the terms R^1B_1, the R^3L, and the NBO_P charge (Figure 2). The NBO_p parameter is likely describing the hydrogen bonding capacity between the catalyst (phosphoric acid) and substrate (the primary or secondary alcohol), since the NBO_p and NBO_O measures are colinear (see Supporting Information for additional models). The minimum width of the R^1 substiuent, R^1B_1, points to the importance of having bulky groups proximal (R^1 and $R^{1'}$ positions) to the phosphoric acid moiety. The length of the R^3 substituent, R^3L, describes the importance of functionalization at the remote (R^2, R^3) positions for fine tuning of site-selectivity.[20] An absence of these features resulted in lower selectivity (Figure 1). These same parameters were also present in previous MLR analyses of CPA-catalyzed enantioselective transformations, indicating that simliar catalyst features required for high enantioselectivity[12e, 17c] are also beneficial for high site-selectivity in this case.

Previous computational models of CPA-catalyzed transformations have highlighted the contribution of steric bulk proximal to the phosphoric acid moiety to high enantioselectivity.[1a, 12d, 12e, 17b, 17c, 19, 20–21] To develop a model for understanding the importance of this catalyst feature in site- selective acylation, we first investigated several CPA catalyzed acylation mechanisms using DFT transition state calculations (see Supporting Information for details). From these calculations, the most energetically favored pathway proceeded by a bifunctional activation of acetic anhydride and substrate simultaneously by the CPA as depicted within Figure 1C. Using these computational results and inspiration from previous structural descriptions of enantioselective CPA transformations, we propose that catalysts without adequate proximal bulk resulted in a less defined catalyst pocket (Figure 1, **5d-5m**). This in turn provides minimal energetic distinction between the transition states leading to **2** and **3** (Figure 1C, top).[1a, 20] In contrast, the presence [1a, 19] of bulky groups shape the catalyst pocket such that differences arise upon association of each alcohol to the phosphoric acid. In considering the acylation of the primary alcohol, steric interactions with the bulky groups on the catalyst reduce the number of low-lying productive conformations. This effect is less pronounced when the secondary alcohol associates with the phosphoric acid, such that there are more productive conformations that avoid steric interactions with 2,6-substituents (Figure 1C, bottom).

An interesting trend emerged from the data obtained within this particular case as a function of variation of R^3 group on observed site-selectivity. Although incorporating R^3 substituents is generally beneficial for site-selectivity as indicated from the R^3L term in the MLR analysis, the effect varied depending on the type of substituent. Aryl groups at R^3 resulted in a dramatic improvement in site-selectivity (**5n** vs **5q** - **5s**) while alkyl groups provided a modest enhancement (**5n** vs **5o**). We hypothesized that the differences in selectivity were the result of attractive NCI's between the remote R^3-phenyl substituent in **5q** and the substrate,

which are not captured by the Sterimol term in the model. Additionally, we reasoned that these NCIs should be present to a greater extent in the transition state leading to **2** than in the transition state leading to **3**. To probe this hypothesis, we performed transition state analysis on the acylation reaction using **5q** and a truncated **1** (see Supporting Information for computational methods). Multiple low-lying TS leading to products **2** and **3** are present. Boltzmann averaging of all TS leading to the formation of **2** and **3** resulted in a computed selectivity of 1.4 kcal/mol, consistent with the experimental results observed (Figure 2, 1.84 kcal/mol, see Supporting Information for details).[22] The relative abundance and strength of attractive NCIs between the relevant sites of interaction within TS2 and TS1 were then assessed using second order perturbation theory (Supporting Information).[21, 23] We found that CH-**π** interactions between the **π** system of the R^3-phenyl of **5q** and the C−H of the substrate are more abundant within TS2 than in TS1 (Supporting Information).

We next investigated the influence that the hydrocarbon framework of **1** has on site-selectivity. To examine this, **6**, a derivative of **1** in which the alkene was removed by hydrogenation, was synthesized and subjected to acylation with the optimized conditions using catalyst **5q**. A substantial decrease in selectivity was observed (8.8:1 for **6** vs 28.1:1 for **1**, Scheme 1). This result prompted us to use TS analysis to assess if this diminished selectivity resulted from weaker or less abundant NCI's between the R^3-phenyl of **5q** and **6**. The calculated TS reproduced the experimental selectivity well (experimental ΔΔG‡ 1.1 kcal/mol, computed ΔΔG‡ 1.0 kcal/ mol). The TS leading to **7** and **8** either completely lack or contain limited weak interactions with the R^3-phenyl of **5q** (Supporting Information). These results indicate that subtle changes in the conformation of the substrate can significantly affect the non-covalent interactions needed for site-selectivity, highlighting the challenges associated with achieving site-selectivity in complex molecules.[24]

As a final step, we sought to expand BINOL-derived CPA-catalyzed site-selective acylation to a different class of natural products with a drastically different framework. Derivatives of flavanoids are under study to optimize their wide range of biological activities, [25] but few examples exist for catalyst- or reagent-controlled[26] site-selective O-functionalization of phenols.[27] We thus targeted the acylation of naringenin, a triphenol-containing flavonoid. Previous literature reports on the acylation and alkylation of narigenin[28] and related flavonoids[29] with various acyl halides[30] leverages the higher acidity of the phenol para to the ketone to achieve site-selectivity (pK_a of C7-OH = 7.5, pK_a of C4'-OH = 8.4).[31] Consistent with this, we found that acylation of **8** under basic conditions is highly selective for the formation of **11** (Table 1, entry 1). Since the mechanism of CPA-catalyzed acylation does not likely involve deprotonation of the phenol prior to acylation (see Supporting Information), we hypothesized that acylation with phosphoric acids could provide a different selectivity profile. Indeed, using diphenylphosphoric acid (DPP) as the catalyst reverses the selectivity, albeit with low reactivity (Table 1, entry 2, 18% yield of acylated products). A higher temperature is required for acylation of the phenols compared to alcohols (45 °C vs 4 °C), but both reactivity and site-selectivity can be enhanced with catalysts **5k** and **5u**. Significant catalyst control of site-selectivity was achieved using the catalyst containing 3,3'-substituents with the bulkiest groups in the 2,3,4,6- positions, giving a selectivity of 7.0:1 for **10** (catalyst **5u**, entry 5).

In summary, BINOL-based chiral phosphoric acids have enabled the site-selective acylation of a diol-containing steroidal natural product. MLR analysis reveals that the same catalyst features that create a defined catalyst pocket required for high enantioselectivity are also required for site-selectivity in this case. DFT calculations point to CH-π interactions between the natural product and catalyst as additional factors contributing to site-selectivity. Both analyses indicate that strategic structural modification of the substituents on the CPA could improve site-selectivity. Furthermore, using this mode of acylation catalyzed by CPAs, we achieved a rare example of site-selective acylation of phenols in a flavonoid natural product. Collectively, these findings suggest that this class of catalysts may have broader applications in site-selective catalysis.

Supplementary Material

Refer to Web version on PubMed Central for supplementary material.

ACKNOWLEDGMENT

S.J.M., M.S.S., and F.D.T. are grateful to the National Institute of General Medical Sciences of the National Institutes of Health for support (GM121383 and GM118190). We thank Aaron Featherston (Yale) for the large-scale synthesis of a catalyst intermediate, and Dr. Brandon Q. Mercado for solving the X-ray crystal structure of **6**. We thank Dr. Jolene P. Reid for her expertise and assistance. We also thank Sophia Robinson (Utah) and Dr. Hyung Yoon (Yale) for their insight. Computational resources were provided by the Center for High Performance Computing at the University of Utah.

REFERENCES

1. (a)Parmar D; Sugiono E; Raja S; Rueping M Complete Field Guide to Asymmetric BINOL-Phosphate Derived Bronsted Acid and Metal Catalysis: History and Classification by Mode of Activation; Bronsted Acidity, Hydrogen Bonding, Ion Pairing, and Metal Phosphates. Chem. Rev 2014, 114, 9047–9153; [PubMed: 25203602] (b)Phipps RJ; Hamilton GL; Toste FD The progression of chiral anions from concepts to applications in asymmetric catalysis. Nat. Chem 2012, 4, 603–614. [PubMed: 22824891]
2. (a)Shugrue CR; Miller SJ Applications of Nonenzymatic Catalysts to the Alteration of Natural Products. Chem. Rev 2017, 117, 11894–11951; [PubMed: 28580785] (b)Site-selective catalysis in Top. Curr. Chem Kawabata T Ed. Springer: Heidelberg, 2016; p VII, 236 pages.
3. Tay JH; Arguelles AJ; DeMars MD; Zimmerman PM; Sherman DH; Nagorny P Regiodivergent Glycosylations of 6-Deoxy-erythronolide B and Oleandomycin-Derived Macrolactones Enabled by Chiral Acid Catalysis. J. Am. Chem. Soc 2017, 139, 8570–8578. [PubMed: 28627172]
4. Wang HY; Blaszczyk SA; Xiao G; Tang W Chiral reagents in glycosylation and modification of carbohydrates. Chem. Soc. Rev 2018, 47, 681–701. [PubMed: 29206256]
5. Giuliano MW; Miller SJ Site-Selective Reactions with Peptide-Based Catalysts. Top Curr. Chem 2016, 372, 157–201. [PubMed: 26307403]
6. (a)Kawabata T; Muramatsu W; Nishio T; Shibata T; Schedel H A catalytic one-step process for the chemo- and regioselective acylation of monosaccharides. J. Am. Chem. Soc 2007, 129, 12890–12895; [PubMed: 17902666] (b)Schedel H; Kan K; Ueda Y; Mishiro K; Yoshida K; Furuta T; Kawabata T Asymmetric desymmetrization of meso-diols by C-2-symmetric chiral 4-pyrrolidinopyridines. Beilstein J. Org. Chem 2012, 8, 1778–1787; [PubMed: 23209512] (c)Yanagi M; Ninomiya R; Ueda Y; Furuta T; Yamada T; Sunazuka T; Kawabata T Organocatalytic Site-Selective Acylation of 10-Deacetylbaccatin III. Chem. Pharm. Bull 2016, 64, 907–912. [PubMed: 26903156]
7. Lee D; Taylor MS Borinic acid-catalyzed regioselective acylation of carbohydrate derivatives. J. Am. Chem. Soc 2011, 133, 3724–7. [PubMed: 21355584]

8. Shimada N; Nakamura Y; Ochiai T; Makino K Catalytic Activation of Cis-Vicinal Diols by Boronic Acids: Site-Selective Acylation of Carbohydrates. Org. Lett 2019, 21, 3789–3794. [PubMed: 31058511]

9. Sun XX; Lee H; Lee S; Tan KL Catalyst recognition of cis-1,2-diols enables site-selective functionalization of complex molecules. Nat. Chem 2013, 5, 790–795. [PubMed: 23965682]

10. (a)Xiao GZ; Cintron-Rosado GA; Glazier DA; Xi BM; Liu C; Liu P; Tang WP Catalytic Site-Selective Acylation of Carbohydrates Directed by Cation-n Interaction. J. Am. Chem. Soc 2017, 139, 4346–4349; [PubMed: 28297601] (b)Blaszczyk SA; Xiao G; Wen P; Hao H; Wu J; Wang B; Carattino F; Li Z; Glazier DA; McCarty BJ; Liu P; Tang W S-Adamantyl Group Directed Site-Selective Acylation: Applications in Streamlined Assembly of Oligosaccharides. Angew. Chem. Int. Ed 2019, 58, 9542–9546.

11. Allen CL; Miller SJ Chiral copper(II) complex-catalyzed reactions of partially protected carbohydrates. Org. Lett 2013, 15, 6178–81. [PubMed: 24274325]

12. (a)Maity P; Pemberton RP; Tantillo DJ; Tambar UK Bronsted Acid Catalyzed Enantioselective Indole Aza-Claisen Rearrangement Mediated by an Arene CH-O Interaction. J. Am. Chem. Soc 2013, 135, 16380–16383; [PubMed: 24164401] (b)Changotra A; Das S; Sunoj RB Reversing Enantioselectivity Using Noncovalent Interactions in Asymmetric Dearomatization of beta-Naphthols: The Power of 3,3 ‘ Substituents in Chiral Phosphoric Acid Catalysts. Org. Lett 2017, 19, 2354–2357; [PubMed: 28418674] (c)Seguin TJ; Wheeler SE Electrostatic Basis for Enantioselective Bronsted-Acid-Catalyzed Asymmetric Ring Openings of meso-Epoxides. ACS Catal. 2016, 6, 2681–2688;(d)Orlandi M; Coelho JAS; Hilton MJ; Toste FD; Sigman MS Parametrization of Non-covalent Interactions for Transition State Interrogation Applied to Asymmetric Catalysis. J. Am. Chem. Soc 2017, 139, 6803–6806; [PubMed: 28475315] (e)Orlandi M; Hilton MJ; Yamamoto E; Toste FD; Sigman MS Mechanistic Investigations of the Pd(0)-Catalyzed Enantioselective 1,1-Diarylation of Benzyl Acrylates. J. Am. Chem. Soc 2017, 139, 12688–12695. [PubMed: 28800230]

13. Harada S; Kuwano S; Yamaoka Y; Yamada K; Takasu K Kinetic Resolution of Secondary Alcohols Catalyzed by Chiral Phosphoric Acids. Angew. Chem. Int. Ed 2013, 52, 10227–10230.

14. For other CPA-catalyzed enantioselective acylations, see:Yang H; Zheng WH Parallel Kinetic Resolution of Unsymmetrical Acyclic Aliphatic syn-1,3-Diols. Org. Lett 2019, 21, 5197–5200; [PubMed: 31247762] (b)Shimoda Y; Yamamoto H Chiral Phosphoric Acid-Catalyzed Kinetic Resolution via Amide Bond Formation. J. Am. Chem. Soc 2017, 139, 6855–6858. [PubMed: 28488440]

15. A competition experiment between a 1:1 molar ratio of neopentyl alcohol and cyclohexanol under CPA-catalyzed acylation gives a ratio of 7.0:1 of the acylation products in favor of neopentyl acetate. See Supporting Information for experimental details.

16. Lewis CA; Miller SJ Site-selective derivatization and remodeling of erythromycin A by using simple peptide-based chiral catalysts. Angew. Chem. Int. Ed. Engl 2006, 45, 5616–9. [PubMed: 16858713]

17. (a)Kwon Y; Li J; Reid JP; Crawford JM; Jacob R; Sigman MS; Toste FD; Miller SJ Disparate Catalytic Scaffolds for Atroposelective Cyclodehydration. J. Am. Chem. Soc 2019, 141, 6698–6705; [PubMed: 30920223] (b)Coelho JAS; Matsumoto A; Orlandi M; Hilton MJ; Sigman MS; Toste FD Enantioselective fluorination of homoallylic alcohols enabled by the tuning of non-covalent interactions. Chem. Sci 2018, 9, 7153–7158; [PubMed: 30310638] (c)Biswas S; Kubota K; Orlandi M; Turberg M; Miles DH; Sigman MS; Toste FD Enantioselective Synthesis of N,S-Acetals by an Oxidative Pummerer-Type Transformation using Phase-Transfer Catalysis. Angew. Chem. Int. Ed 2018, 57, 589–593;(d)Yamamoto E; Hilton MJ; Orlandi M; Saini V; Toste FD; Sigman MS Development and Analysis of a Pd(0)-Catalyzed Enantioselective 1,1-Diarylation of Acrylates Enabled by Chiral Anion Phase Transfer. J. Am. Chem. Soc 2016, 138, 15877–15880; [PubMed: 27960315] (e)Milo A; Neel AJ; Toste FD; Sigman MS A data-intensive approach to mechanistic elucidation applied to chiral anion catalysis. Science 2015, 347, 737–743. [PubMed: 25678656]

18. Santiago CB; Guo JY; Sigman MS Predictive and mechanistic multivariate linear regression models for reaction development. Chem. Sci 2018, 9, 2398–2412. [PubMed: 29719711]

19. (a)Reid JP; Sigman MS Comparing quantitative prediction methods for the discovery of small-molecule chiral catalysts. Nat. Rev. Chem 2018, 2, 290–305;(b)Sigman MS; Harper KC; Bess EN; Milo A The Development of Multidimensional Analysis Tools for Asymmetric Catalysis and Beyond. Acc. Chem. Res 2016, 49, 1292–1301. [PubMed: 27220055]

20. Reid JP; Goodman JM Goldilocks Catalysts: Computational Insights into the Role of the 3,3 ‘ Substituents on the Selectivity of BINOL-Derived Phosphoric Acid Catalysts. J. Am. Chem. Soc 2016, 138, 7910–7917. [PubMed: 27227372]

21. Maji R; Mallojjala SC; Wheeler SE Chiral phosphoric acid catalysis: from numbers to insights. Chem. Soc. Rev 2018, 47, 1142–1158. [PubMed: 29355873]

22. Peng Q; Duarte F; Paton RS Computing organic stereoselectivity - from concepts to quantitative calculations and predictions. Chem. Soc. Rev 2016, 45, 6093–6107. [PubMed: 27722685]

23. (a)Reed AE; Curtiss LA; Weinhold F Intermolecular Interactions from a Natural Bond Orbital, Donor-Acceptor Viewpoint. Chem. Rev 1988, 88, 899–926;(b)Weinhold F Natural bond orbital analysis: A critical overview of relationships to alternative bonding perspectives. J. Comput. Chem 2012, 33, 2363–2379. [PubMed: 22837029]

24. Another challenge associated with site-selective functionalizations is achieving selectivity for all reactive sites. In this case, we were not able to obtain site-selectivity for 3 with this catalyst system.

25. (a)Leonardi T; Vanamala J; Taddeo SS; Davidson LA; Murphy ME; Patil BS; Wang NY; Carroll RJ; Chapkin RS; Lupton JR; Turner ND Apigenin and naringenin suppress colon carcinogenesis through the aberrant crypt stage in azoxymethane-treated rats. Exp. Biol. Med 2010, 235, 710–717;(b)Tripoli E; La Guardia M; Giammanco S; Di Majo D; Giammanco M Citrus flavonoids: Molecular structure, biological activity and nutritional properties: A review. Food Chem. 2007, 104, 466–479;(c)Celiz G; Daz M; Audisio MC Antibacterial activity of naringin derivatives against pathogenic strains. J. Appl. Microbiol 2011, 111, 731–738; [PubMed: 21672094] (d)Cushnie TPT; Lamb AJ Antimicrobial activity of flavonoids. Int. J. Antimicrob. Ag 2005, 26, 343–356.

26. Fatykhov RF; Khalymbadzha IA; Chupakhin ON; Charushin VN; Inyutina AK; Slepukhin PA; Kartsev VG 1-Nicotinoylbenzotriazole: A Convenient Tool for Site-Selective Protection of 5,7-Dihydroxycoumarins. Synthesis 2019.

27. For examples of the complementary catalytic enantioselective desymmetrizations of bis(phenols), see:Lewis CA; Gustafson JL; Chiu A; Balsells J; Pollard D; Murry J; Reamer RA; Hansen KB; Miller SJ A Case of Remote Asymmetric Induction in the Peptide-Catalyzed Desymmetrization of a Bis(phenol). J. Am. Chem. Soc 2008, 130, 16358–16365. [PubMed: 19006301]

28. Yoon H; Kim TW; Shin SY; Park MJ; Yong Y; Kim DW; Islam T; Lee YH; Jung KY; Lim Y Design, synthesis and inhibitory activities of naringenin derivatives on human colon cancer cells. Bioorg. Med. Chem. Lett 2013, 23, 232–238. [PubMed: 23177257]

29. Jeong TS; Kim EE; Lee CH; Oh JH; Moon SS; Lee WS; Oh GT; Lee S; Bok SH Hypocholesterolemic activity of hesperetin derivatives. Bioorg. Med. Chem. Lett 2003, 13, 2663–2665. [PubMed: 12873489]

30. Davis BD; Needs PW; Kroon PA; Brodbelt JS Identification of isomeric flavonoid glucuronides in urine and plasma by metal complexation and LC-ESI-MS/MS. J. Mass. Spectrom 2006, 41, 911–920. [PubMed: 16810646]

31. Musialik M; Kuzmicz R; Pawlowski TS; Litwinienko G Acidity of hydroxyl groups: an overlooked influence on antiradical properties of flavonoids. J. Org. Chem 2009, 74, 2699–709. [PubMed: 19275193]

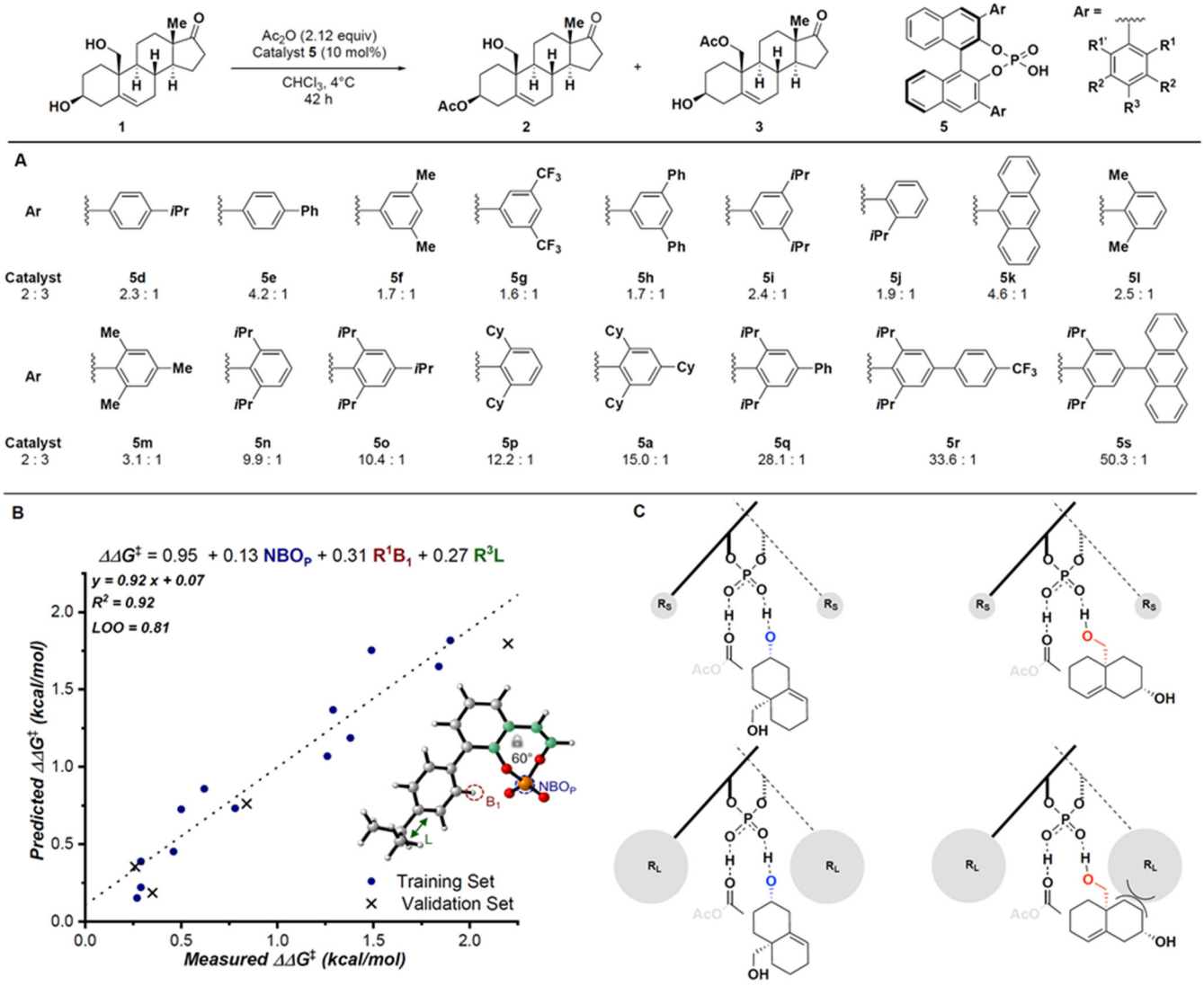

Figure 1.

A) Panel of CPAs tested and selectivities obtained. B) MLR model for site selective acylation. C) Rationale for site-selectivity using catalysts with small proximal substituents (top, $R^1 = R^{1'} = H$) and large proximal substituents (bottom, $R^1 = R^{1'} \neq H$).

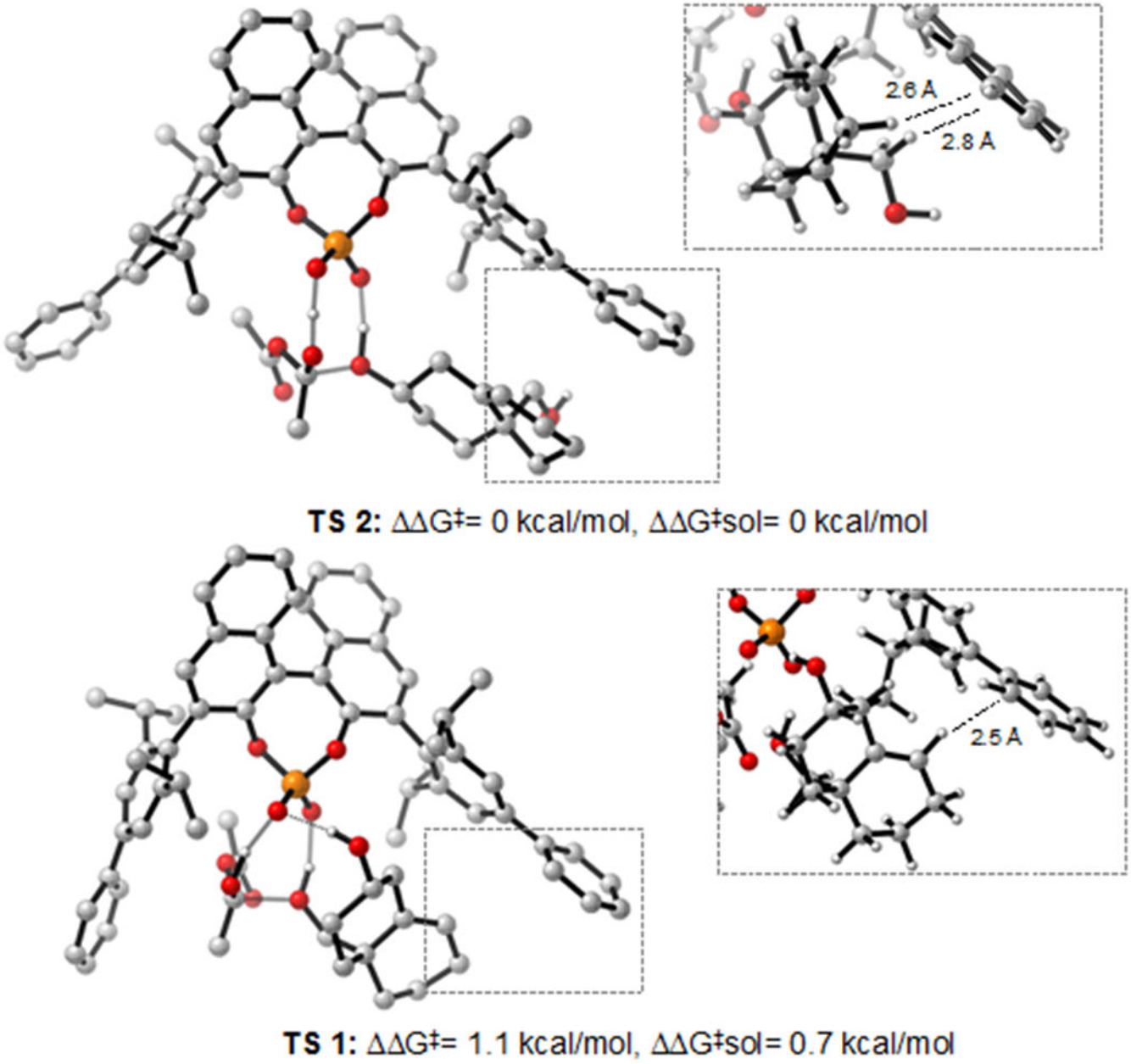

Figure 2.

Transition state structures for the formation of **2** (TS 2, top) and **3** (TS1, bottom). The energies presented are for these TS, demonstrating the underestimated selectivity observed when comparing the lowest energy TS. Geometries were obtained at a ω-B97XD/6-31G* level of theory and single-point energies from M06-2X/def2-SVP.

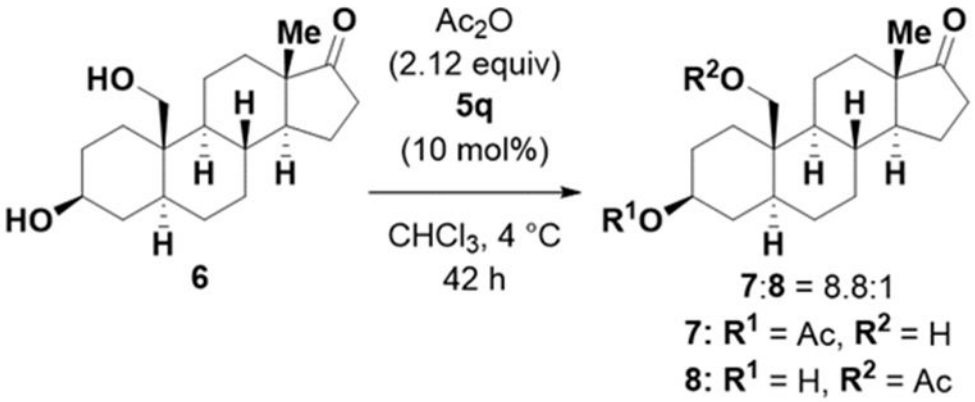

	ΔΔG‡ (kcal/mol)
Experimental	1.1
Calculated	1.0

Scheme 1.
Acylation of saturated steroid 6.

Table 1.

Reaction optimization for the site-selective acylation of 19-OH-DHEA, 1.

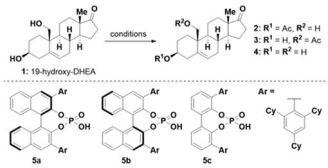

Entry	Conditions	2 : 3 : 4 (% yields)[a]	2 : 3
1	Ac_2O, DMAP, NEt_3, rt	20 : 24 : 21	0.8 : 1
2	Ac_2O, DPP (25 mol%), rt	24 : 20 : 21	1.2 : 1
3	Ac_2O, **5a** (10 mol%), rt	56 : 7 : 10	8.5 : 1
4	Ac_2O, **5b** (10 mol%), rt	13 : 5 : 1	2.9 : 1
5	Ac_2O, **5c** (10 mol%), rt	29 : 8 : 6	3.4 : 1
6	Ac_2O, **5c** (10 mol%), 4 °C	34.7 : 2.3 : 1.8[b]	15 : 1

[a] Yields were determined by HPLC at 214 nm with *N*-phenylacetamide as internal standard.

[b] Average of two runs. DPP = diphenylphosphoric acid, rt = room temperature.

Table 2.

Site-selective acylation of naringenin.

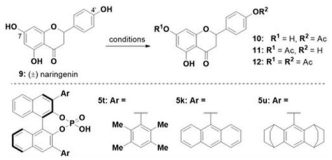

Entry	Conditions	10 : 11 : 12 (% yields)[a]	10 : 11
1	AcCl, K_2CO_3, MeCN, rt	2 : 65 : 13	1 : 33
2	Ac_2O, DPP, EtOAc, 45 °C	14 : 4 : 0	3.5 : 1
3	Ac_2O, **5t**, EtOAc, 45 °C	20 : 8 : 3	2.5 : 1
4	Ac_2O, **5k**, EtOAc, 45 °C	26 : 5 : 2	5.2 : 1
5[b]	Ac_2O, **5u**, EtOAc, 45 °C	35 : 5 : 3	7.0 : 1

[a]Yields were determined by HPLC at 230 nm with *N*-phenylacetamide as internal standard.

[b]**10, 11,** and unreacted **9** were racemic.